

## Article

# Investigation on Application Prospect of Refractories for Hydrogen Metallurgy: The Enlightenment from the Reaction between Commercial Brown Corundum and Hydrogen

Shaofei Li , Ding Chen \*, Huazhi Gu, Ao Huang and Lvping Fu

The State Key Laboratory of Refractories and Metallurgy, Wuhan University of Science and Technology, Wuhan 430081, China

\* Correspondence: chending\_his@163.com; Tel./Fax: +86-27-68862160

**Abstract:** Hydrogenous environments put forward new requirements to refractories for the hydrogen metallurgy field. The temperature and impurities in refractories played an important role in stability. A commercial brown corundum with many impurities was adopted as a raw material, thermodynamic calculations and reduction experiments of the brown corundum by high-purity hydrogen (99.99%) were accepted to investigate the stability of the oxides. The weight loss and mass fraction were tested to estimate the stability of the oxides in the brown corundum. XRD and SEM were used to analyze the mineral compositions and microstructures. The results showed that: the thermodynamic stability of the oxides in the brown corundum under high-purity hydrogen was in the order of  $\text{Al}_2\text{O}_3 > \text{CaO} > \text{MgO} > \text{SiO}_2 > \text{TiO}_2 > \text{Fe}_2\text{O}_3$  at temperatures lower than 1400 °C. Obvious weight loss appeared after heating at 1400 °C for 8 h. The content of CaO did not decline after reduction even at 1800 °C, owing to the formation of hibonite ( $\text{CaAl}_{12}\text{O}_{19}$ ), high-purity  $\text{Al}_2\text{O}_3$  and  $\text{CaAl}_{12}\text{O}_{19}$ -based refractories had the prospect for lining materials in the hydrogen metallurgy field, owing to their excellent chemical stability under hydrogenous environments.



**Citation:** Li, S.; Chen, D.; Gu, H.; Huang, A.; Fu, L. Investigation on Application Prospect of Refractories for Hydrogen Metallurgy: The Enlightenment from the Reaction between Commercial Brown Corundum and Hydrogen. *Materials* **2022**, *15*, 7022. <https://doi.org/10.3390/ma15197022>

Academic Editor: Jacques Huot

Received: 21 September 2022

Accepted: 6 October 2022

Published: 10 October 2022

**Publisher's Note:** MDPI stays neutral with regard to jurisdictional claims in published maps and institutional affiliations.



**Copyright:** © 2022 by the authors. Licensee MDPI, Basel, Switzerland. This article is an open access article distributed under the terms and conditions of the Creative Commons Attribution (CC BY) license (<https://creativecommons.org/licenses/by/4.0/>).

**Keywords:**  $\text{Al}_2\text{O}_3$  based refractories; brown corundum; chemical stability; hydrogen metallurgy

## 1. Introduction

The process of iron ore reduction by carbon in iron and steel metallurgy has contributed the most greenhouse gas emissions in the whole process of iron and steel production.  $\text{CO}_2$  emissions from the steel industry have constituted a high proportion, equivalent to about 33.8% of industrial emissions [1]. The enhancement of clean energy technology and optimizing energy structures are crucial for carbon emissions reduction [2]. Therefore, environmentally friendly and economical iron ore reduction methods have become a hot spot in the exploration of an ideal process. Hydrogen metallurgy is a technology that partially or completely uses hydrogen to replace carbon as the reduction agent to reduce iron ore to obtain solid iron at the temperature range below the melting point of Fe, which has been very beneficial through energy savings and the reduction in  $\text{CO}_2$  emissions [3].

Refractories were indispensable key materials in the iron and steel industry, the hydrogenous environment has put forward new requirements due to the strong reducibility of hydrogen. Tso [4] has studied reactions between fused silica and hydrogen gas in the temperature range from 1200 °C to 1400 °C, the formation of  $\text{SiO}$  (g) and  $\text{H}_2\text{O}$  (g) has caused the main weight loss. Herbell [5] has investigated the reactions between dry/wet hydrogen and some high-temperature ceramics including  $\text{Al}_2\text{O}_3$ ,  $\text{MgO}$ ,  $\text{SiC}$ ,  $\text{Si}_3\text{N}_4$  and mullite at 1400 °C, the increase in moisture provided the most benefits for stability, the  $\text{Al}_2\text{O}_3$  ceramic performed excellently in stability. However, the reaction of  $\text{Al}_2\text{O}_3$ -based ceramics with hydrogen at the temperature range over 1400 °C needs further research.

Presently, blast furnace ironmaking adding hydrogen and direct reduction iron by hydrogen (DRI) are the two main hydrogen metallurgy methods [6,7], the temperature of

the former process is about 1500 °C, the DRI is 750–1360 °C [8–16]. In addition, raising the temperature is the trend because a high temperature means high productivity in the hydrogen metallurgy process. So, the stability of Al<sub>2</sub>O<sub>3</sub>-based materials under a hydrogen atmosphere in a wide temperature range should be studied. Furthermore, the presence of impurities has played a significant role in the stability of the refractories and high-temperature ceramics under a hydrogen atmosphere.

Commercial corundum raw materials including brown corundum, white corundum, and tabular corundum are the main Al<sub>2</sub>O<sub>3</sub>-based refractory raw materials. In general, the content of Al<sub>2</sub>O<sub>3</sub> in the latter two corundum raw materials is close to 99%. There are many impurities in brown corundum. In this paper, the commercial brown corundum was adopted as a raw material to react with the high-purity hydrogen in a wide temperature range from 600 °C to 1800 °C. The mass fractions of the oxides and mineral phase changes were tested to estimate the stability of the oxides in the brown corundum. The results have been beneficial for seeking stable refractories for the hydrogen metallurgy field.

## 2. Materials and Methods

Commercial brown corundum powder ( $\leq 0.045$  mm) was chosen as the raw material. The chemical compositions are shown in Table 1, the raw material consisted of 92.97 wt% of Al<sub>2</sub>O<sub>3</sub> and some impurities including SiO<sub>2</sub>, CaO, TiO<sub>2</sub> and MgO. The XRD pattern (Figure 1) showed the mineralogical compositions of the raw material, Al<sub>2</sub>O<sub>3</sub> (corundum) was the main mineral phase. The peaks of the minerals related to the impurities are not shown in Figure 1, which might be caused by the following two reasons. First, the amount of such minerals containing impurities was too little. Second, impurities were distributed in the amorphous glass phases. High-purity hydrogen (99.99% of volume fraction) was adopted as the reductive agent.

**Table 1.** Chemical compositions of the brown corundum raw materials (wt%).

SiO <sub>2</sub>	Al <sub>2</sub> O <sub>3</sub>	Fe <sub>2</sub> O <sub>3</sub>	CaO	MgO	K <sub>2</sub> O	Na <sub>2</sub> O	TiO <sub>2</sub>
1.12	92.97	0.2	0.26	0.17	0.094	0.038	2.13

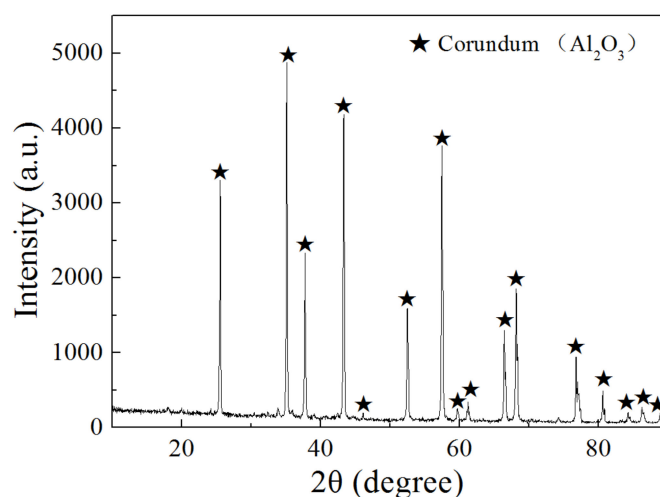


**Figure 1.** XRD pattern of the brown corundum raw material.

The brown corundum was placed in molybdenum crucibles. The brown corundum raw material was dried at 110 °C for 24 h in a vacuum oven. The samples were ready for experiments after drying. Then the crucibles containing the brown corundum raw materials were put into a high temperature hydrogen furnace and heated to 600 °C, 700 °C, 800 °C, 1200 °C, 1400 °C, 1600 °C and 1800 °C for 8 h, respectively, under the high-purity

hydrogen atmosphere. The heating rate was 3~6 °C/min, the flow rate of hydrogen was 2500 mL/min.

The masses of the brown corundum before and after heating were measured accurately. The weight loss of the brown corundum was evaluated as follows:

$$\text{Weight loss} = (M - M_0)/M_0 \quad (1)$$

Therein,  $M_0$  is the mass of a molybdenum crucible containing the brown corundum raw material before heating,  $M$  is the mass of a molybdenum crucible containing the brown corundum raw material after heating at different temperatures.

Then, the mass fractions of the  $\text{Al}_2\text{O}_3$  and main impurities including  $\text{SiO}_2$ ,  $\text{Fe}_2\text{O}_3$ ,  $\text{CaO}$ ,  $\text{TiO}_x$ ,  $\text{MgO}$  in the brown corundum were measured via XRF (X-ray Fluorescence). The microstructures and mineralogical compositions were tested via SEM (SEM, JSM-6610, JEOL, Tokyo, Japan) and X-ray diffraction (XRD, X' Pert Pro, Philips, The Netherlands).

### 3. Results and Discussion

#### 3.1. Thermodynamic Calculations

The oxides in the brown corundum could react with the hydrogen, which would form gaseous products and result in weight loss. The equilibrium partial pressure of the gaseous products could be calculated. The reaction between  $\text{SiO}_2$  and  $\text{H}_2$  was taken as an example. Equation (2) showed the reaction, and the equilibrium partial pressures of  $\text{SiO}$  (g) and  $\text{H}_2\text{O}$  (g) could be calculated according to Equation (3) under the hydrogen atmosphere [4]. For Equation (3), the pressure of  $\text{H}_2$  and the value of  $P^\theta$  were both  $10^5$  Pa. The results were obtained and are shown in Table 2, the equilibrium partial pressures of  $\text{SiO}$  (g) and  $\text{H}_2\text{O}$  (g) were both 2.7 Pa at 1200 °C, which would cause a slight weight loss of the brown corundum. At 1600 °C, the value was 345.2 Pa, which indicated serious degradation of  $\text{SiO}_2$  in the hydrogen furnace.



$$\ln \frac{\frac{P_{\text{SiO}}}{P^\theta} \cdot \frac{P_{\text{H}_2\text{O}}}{P^\theta}}{\frac{P_{\text{H}_2}}{P^\theta}} = \frac{\Delta_r G_m^\theta}{-RT} \quad (3)$$

**Table 2.** Equilibrium partial pressures of gaseous products of reactions at different temperatures (Pa).

Reactions		1200 °C	1400 °C	1600 °C	1800 °C
$\text{SiO}_2 (\text{s}) + \text{H}_2 (\text{g}) = \text{SiO} (\text{g}) + \text{H}_2\text{O} (\text{g})$	$P_{\text{SiO}}$	2.7	41.3	345.2	1884.3
	$P_{\text{H}_2\text{O}}$	2.7	41.3	345.2	1884.3
$\text{MgO} (\text{s}) + \text{H}_2 (\text{g}) = \text{Mg} (\text{g}) + \text{H}_2\text{O} (\text{g})$	$P_{\text{Mg}}$	2.2	23.2	146.2	639.4
	$P_{\text{H}_2\text{O}}$	2.2	23.2	146.2	639.4
$\text{Al}_2\text{O}_3 (\text{s}) + 3\text{H}_2 (\text{g}) = 2\text{Al} (\text{g}) + 3\text{H}_2\text{O} (\text{g})$	$P_{\text{Al}}$	$9.3 \times 10^{-22}$	$7.0 \times 10^{-18}$	$7.5 \times 10^{-15}$	$2.0 \times 10^{-12}$
	$P_{\text{H}_2\text{O}}$	$1.4 \times 10^{-21}$	$1.0 \times 10^{-17}$	$1.1 \times 10^{-14}$	$3.0 \times 10^{-12}$
$\text{CaO} (\text{s}) + \text{H}_2 (\text{g}) = \text{Ca} (\text{g}) + \text{H}_2\text{O} (\text{g})$	$P_{\text{Ca}}$	0.3	2.0	11.6	60.9
	$P_{\text{H}_2\text{O}}$	0.3	2.0	11.6	60.9
$2\text{TiO}_2 (\text{s}) + \text{H}_2 (\text{g}) = \text{Ti}_2\text{O}_3 (\text{s}) + \text{H}_2\text{O} (\text{g})$	$P_{\text{H}_2\text{O}}$	77.4	201.7	394.1	625.5
$\text{Fe}_2\text{O}_3 (\text{s}) + 3\text{H}_2 (\text{g}) = 2\text{Fe} + 3\text{H}_2\text{O} (\text{g})$	$P_{\text{H}_2\text{O}}$	$1.5 \times 10^5$	$1.3 \times 10^5$	$9.8 \times 10^4$	$7.3 \times 10^4$

The reaction conditions of the other oxides were calculated via the same method and the results are shown in Table 2.

$\text{Al}_2\text{O}_3$  was the most stable oxide in the brown corundum, the equilibrium partial pressures of  $\text{Al}$  (g) and  $\text{H}_2\text{O}$  (g) were  $2.0 \times 10^{-12}$  Pa and  $3.0 \times 10^{-12}$  Pa at 1800 °C, such a small sum of gaseous products had a negligible effect on mass.  $\text{CaO}$  also performed well in stability when the temperature was lower than 1600 °C. The reduction process of  $\text{TiO}_2$  was complicated, a series of oxides of titanium would be generated [17,18],  $\text{Ti}_2\text{O}_3$  was accepted as a reduction product for the calculation in Table 2. The  $\text{TiO}_x$  ( $x \leq 2$ ) was adopted to stand for

oxides of titanium in the following contents. The thermodynamic stability of the oxides under high-purity hydrogen was in the order of  $\text{Al}_2\text{O}_3 > \text{CaO} > \text{MgO} > \text{SiO}_2 > \text{TiO}_2 > \text{Fe}_2\text{O}_3$  at the temperature lower than  $1400\text{ }^\circ\text{C}$ , continuously increasing the temperature, the  $\text{SiO}_2$  performed worse in stability, compared with  $\text{TiO}_2$  and  $\text{MgO}$ . The  $\text{Al}_2\text{O}_3$  could remain stable even at  $1800\text{ }^\circ\text{C}$ .

### 3.2. Weight Loss of Brown Corundum

The  $\text{Al}_2\text{O}_3$  in the brown corundum was stable under the  $\text{H}_2$  atmosphere according to Table 2. However, the brown corundum raw material consisted of impurities. Some impurities could react with  $\text{H}_2$  at elevated temperatures, which resulted in weight loss. The weight loss of the brown corundum after a high temperature hydrogen reduction is shown in Figure 2. The slight weight loss occurred when the temperature was increased to  $1200\text{ }^\circ\text{C}$ , which may be caused by the reduction in  $\text{Fe}_2\text{O}_3$ . Continuously raising the temperature to  $1400\text{ }^\circ\text{C}$  resulted in the increase in weight loss, the reduction in  $\text{TiO}_2$ ,  $\text{MgO}$  and  $\text{SiO}_2$  contributed a lot for weight loss.

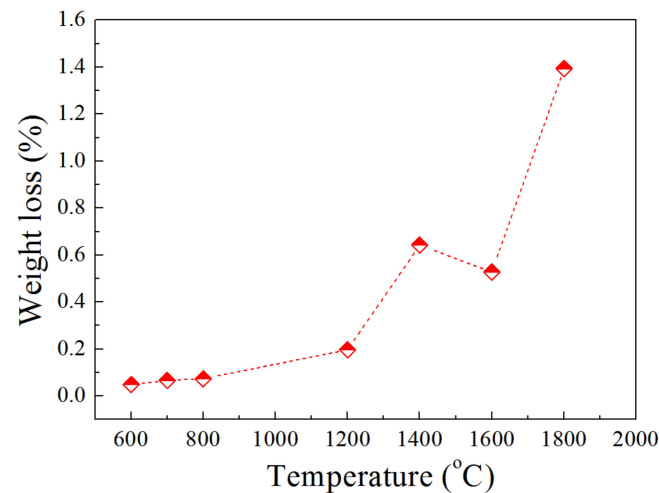


**Figure 2.** Weight loss of the brown corundum after reaction with high-purity hydrogen at different temperatures.

The mass fractions of  $\text{Al}_2\text{O}_3$  and impurities were tested and are shown in Figure 3. On the whole, the content of the  $\text{Al}_2\text{O}_3$  presented an upward trend (shown in Figure 3a). Some impurities reacted with the  $\text{H}_2$ , the gaseous products volatilized, while the  $\text{Al}_2\text{O}_3$  had favorable stability in the high-temperature hydrogen furnace, which could have resulted in the increase in mass fraction of the  $\text{Al}_2\text{O}_3$  and the decrease in mass fractions of the impurities. The mass fractions of the impurities after reduction for 8 h at different temperatures are shown in Figure 3b, the obvious mass fraction change occurred after rising up to  $1400\text{ }^\circ\text{C}$ , the mass fractions of  $\text{TiO}_x$  and  $\text{CaO}$  performed upward trends. The reaction between  $\text{Fe}_2\text{O}_3$  and  $\text{H}_2$  could proceed at a low temperature according to Table 2, the contents of  $\text{Fe}_2\text{O}_3$  decreased from  $600\text{ }^\circ\text{C}$  to  $1200\text{ }^\circ\text{C}$ , a continuously rising temperature accelerated the decline of  $\text{Fe}_2\text{O}_3$ . When the temperature was increased to  $1400\text{ }^\circ\text{C}$ , the mass fraction of  $\text{SiO}_2$  decreased obviously. On the whole, the  $\text{Al}_2\text{O}_3$  was stable during heating under a hydrogen atmosphere up to  $1800\text{ }^\circ\text{C}$ . Furthermore, the  $\text{CaO}$  and  $\text{TiO}_x$  also performed excellently in stability during the experiments.  $\text{TiO}_2$  was easily reduced by  $\text{H}_2$  below  $1600\text{ }^\circ\text{C}$ , according to Table 2. However, the reduction product was solid phase  $\text{TiO}_x$  ( $x \leq 2$ ) with a high melting point. In the case of  $\text{Ti}_2\text{O}_3$ , the  $\text{Ti}_2\text{O}_3$  had excellent stability under a hydrogen atmosphere. Equation (4) showed the reaction between the  $\text{Ti}_2\text{O}_3$  and  $\text{H}_2$ , the equilibrium partial pressure of  $\text{H}_2\text{O}$  (g) could be calculated based on Equation (5), the value was  $0.18\text{ Pa}$  at  $1800\text{ }^\circ\text{C}$ , which indicated a insignificant degradation of  $\text{Ti}_2\text{O}_3$  under

the hydrogen atmosphere at 1800 °C. The oxides of titanium performed an upward trend of mass fraction, with the increasing of temperature owing to the stability of  $TiO_x$ .



$$\ln \frac{\frac{P_{H_2O}}{p^\theta}}{\frac{P_{H_2}}{p^\theta}} = \frac{\Delta_r G_m^\theta}{-RT} \quad (5)$$

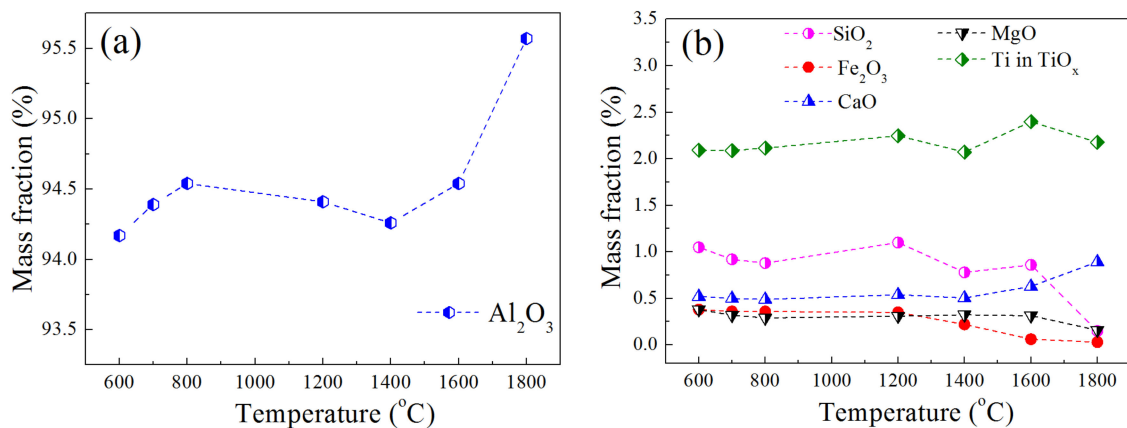


**Figure 3.** Mass fractions of different oxides in brown corundum after reaction with high-purity hydrogen at different temperatures: (a)  $Al_2O_3$  and (b) impurity oxides.

### 3.3. Phase Compositions of Brown Corundum after Reduction by Hydrogen

The mineral phases in brown corundum would change owing to the decrease in impurities. The main phases in the raw material were  $Al_2O_3$  (corundum), based on Figure 1. After the reaction with hydrogen at 1600 °C for 8 h, no peaks containing impurities appeared. When increasing the reaction temperature to 1800 °C, a new mineralogical phase hibonite ( $CaAl_{12}O_{19}$ ) was generated (shown in Figure 4b). According to Table 2,  $CaO$  could be reduced by  $H_2$  at 1800 °C, the pressure of the product  $H_2O$  (g) was 60.9 Pa. The reason that the  $CaO$  content did not decline may be the formation of hibonite ( $CaAl_{12}O_{19}$ ). As shown in Table 3, the pressures of  $Ca$  (g) and  $H_2O$  (g) caused by the reaction between  $CaAl_{12}O_{19}$  and  $H_2$  (g) were just 1.62 Pa at 1800 °C, the partial pressures of the gaseous products were much lower than the reaction of  $CaO$  and  $H_2$  (g), which meant a good stability of hibonite ( $CaAl_{12}O_{19}$ ).

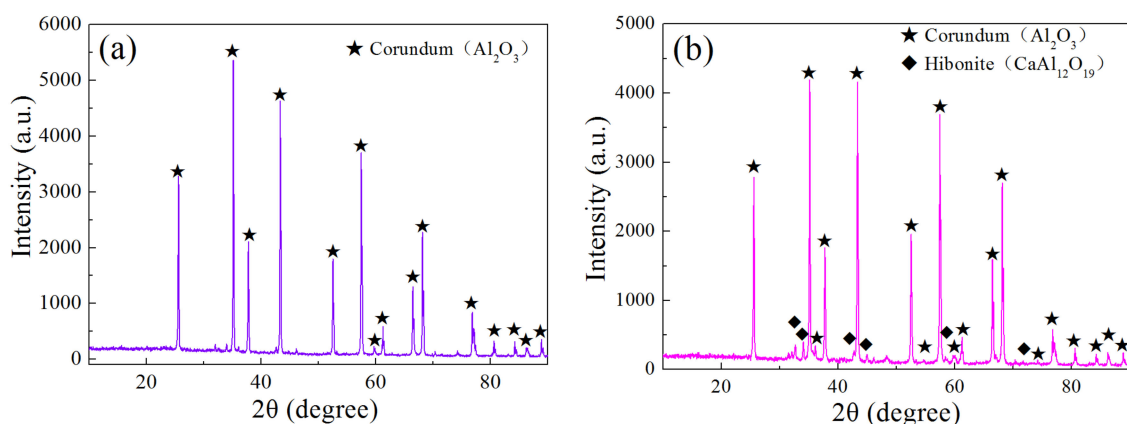


**Figure 4.** XRD patterns of brown corundum after reaction with high-purity hydrogen at different temperatures: (a) 1600 °C and (b) 1800 °C.

**Table 3.** Equilibrium partial pressures of gaseous products of reduction reactions of  $\text{CaAl}_{12}\text{O}_{19}$  and  $\text{CaO}$  at different temperatures (Pa).

Reactions		1200 °C	1400 °C	1600 °C	1800 °C
$\text{CaAl}_{12}\text{O}_{19} (\text{s}) + \text{H}_2 (\text{g}) = \text{Ca} (\text{g}) + \text{H}_2\text{O} (\text{g}) + 6\text{Al}_2\text{O}_3$	$P_{\text{Ca}}$	$3.6 \times 10^{-3}$	$4.7 \times 10^{-2}$	0.35	1.62
	$P_{\text{H}_2\text{O}}$	$3.6 \times 10^{-3}$	$4.7 \times 10^{-2}$	0.35	1.62
$\text{CaO} (\text{s}) + \text{H}_2 (\text{g}) = \text{Ca} (\text{g}) + \text{H}_2\text{O} (\text{g})$	$P_{\text{Ca}}$	0.3	2.0	11.6	60.9
	$P_{\text{H}_2\text{O}}$	0.3	2.0	11.6	60.9

With the increasing of temperature, the contents of  $\text{SiO}_2$  decreased owing to the reduction reaction by hydrogen. The decrease in the  $\text{SiO}_2$  content in the amorphous glass phase was the concrete expression.  $\text{SiO}_2$  in the glass phase transferred to  $\text{SiO} (\text{g})$ , the volatilization of the gaseous products resulted in weight loss.  $\text{Al}_2\text{O}_3$  (corundum) and  $\text{CaAl}_{12}\text{O}_{19}$  (hibonite) were stable under the hydrogen atmosphere even at 1800 °C.  $\text{Al}_2\text{O}_3$  and  $\text{CaAl}_{12}\text{O}_{19}$ -based refractories were suitable for hydrogen metallurgy progress owing to their stability and availability of the raw materials.

### 3.4. Microstructure Evaluation of Brown Corundum after Reduction by Hydrogen

The microstructures of the samples were tested, the morphology and the EDS of the corundum materials are shown in Figure 5, the amorphous glass was distributed between the corundum particles, which consisted of the elements Ti, Al, Si, Mg, K, Fe and O, according to Figure 5d.

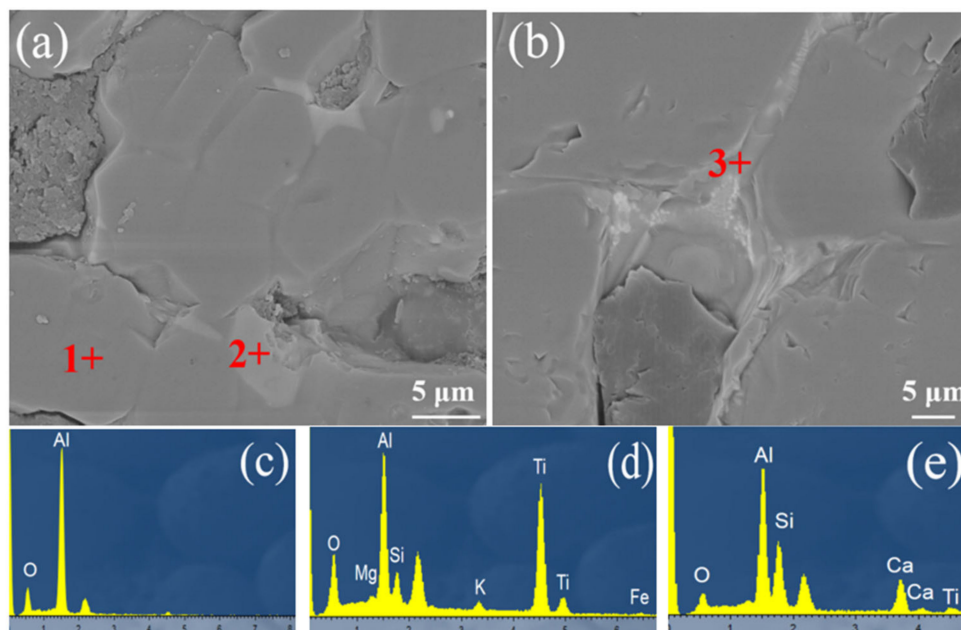


**Figure 5.** SEM photo of brown corundum materials (a) raw materials without reduction, (b) brown corundum after reduction by hydrogen at 1600 °C for 8 h, (c–e) are EDS of point 1, point 2 and point 3, respectively.

After heating at 1600 °C for 8 h in the hydrogen furnace, the compositions of the amorphous glass changed, the peaks of K, Fe and Mg disappeared. The elements Al, Ca, Ti, Si and O made up the amorphous glass based on Figure 5e. Compared with the raw materials, the elements Fe, Mg, and K decreased obviously owing to the reduction by hydrogen during heating at 1600 °C, the  $\text{SiO}_2$  impurities were still distributed between the corundum particles.

With continuous increasing of the temperature to 1800 °C, the phase compositions changed, according to Figure 6. The phases between corundum consisted of the elements

Al, Ti, Ca and O. The element Si could not be detected, which indicated a violent reaction between  $\text{SiO}_2$  and hydrogen at  $1800\text{ }^\circ\text{C}$ . An amorphous glass of  $\text{TiO}_x\text{-Al}_2\text{O}_3\text{-CaO}$  existed in the interface of the corundum particles. Furthermore, lamellar hibonite formed (Figure 6c), some  $\text{TiO}_x$  solubilized in the hibonite, according the result of EDS in point 4 (Figure 6e). The results indicated that the hibonite and corundum were the stable mineral phases under the hydrogen atmosphere, even at an elevated temperature of  $1800\text{ }^\circ\text{C}$ .

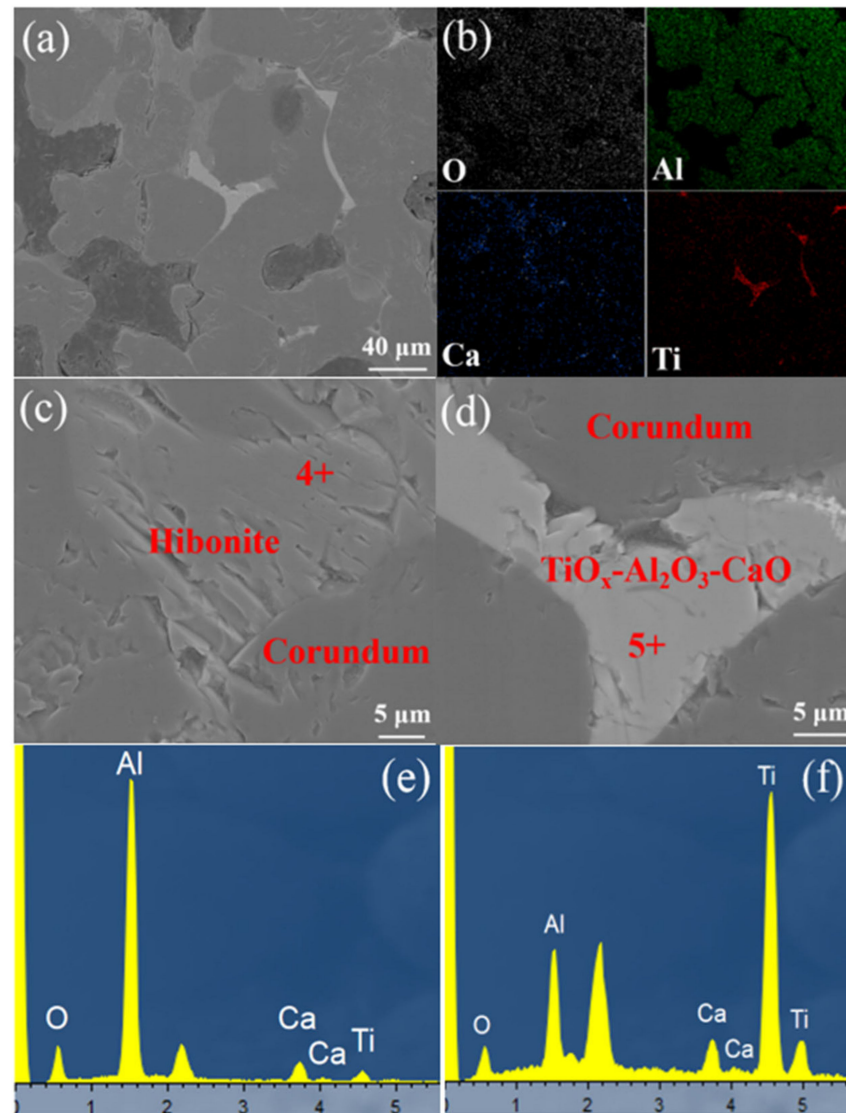


**Figure 6.** SEM photos of brown corundum after reduction by hydrogen at  $1800\text{ }^\circ\text{C}$  for 8 h: (a) microstructure, (b) EDS mapping of (a,c,d) are enlarged views of (a,e,f) are EDS of point 4 and point 5, respectively.

#### 4. Conclusions

For the purpose of seeking suitable refractories for the hydrogen metallurgy field, thermodynamic calculations and reduction experiments of commercial brown corundum by high-purity hydrogen were adopted to investigate the stability of the oxides. The following results were obtained.

- (1) The thermodynamic stability of the oxides under high-purity hydrogen was in the order of  $\text{Al}_2\text{O}_3 > \text{CaO} > \text{MgO} > \text{SiO}_2 > \text{TiO}_2 > \text{Fe}_2\text{O}_3$  at the temperature lower than  $1400\text{ }^\circ\text{C}$ , when continuously increasing the temperature, the  $\text{SiO}_2$  performed worse in stability compared with  $\text{TiO}_2$  and  $\text{MgO}$ . The  $\text{Al}_2\text{O}_3$  could remain stable even at

- 1800 °C. Obvious weight loss appeared when raising the temperature to 1400 °C. The reduction in Fe<sub>2</sub>O<sub>3</sub>, SiO<sub>2</sub> and MgO contributed a lot to the weight loss.
- (2) The pressures of Ca (g) and H<sub>2</sub>O (g) caused by the reaction between CaAl<sub>12</sub>O<sub>19</sub> and H<sub>2</sub> (g) was just 1.62 Pa at 1800 °C. The CaO contents in the brown corundum remained stable owing to the formation of hibonite (CaAl<sub>12</sub>O<sub>19</sub>).
  - (3) The corundum (Al<sub>2</sub>O<sub>3</sub>) and hibonite (CaAl<sub>12</sub>O<sub>19</sub>) performed excellently in stability under the high-purity hydrogen atmosphere, even at 1800 °C, which indicated that high-purity Al<sub>2</sub>O<sub>3</sub> and CaAl<sub>12</sub>O<sub>19</sub>-based refractories were suitable for lining materials in the hydrogen metallurgy field.

**Author Contributions:** Conceptualization, S.L.; methodology, D.C. and L.F.; software, D.C.; validation, D.C.; formal analysis, D.C.; investigation, S.L.; resources, H.G. and A.H.; data curation, S.L.; writing—original draft preparation, S.L.; writing—review and editing, D.C.; visualization, D.C.; supervision, A.H.; project administration, H.G.; funding acquisition, L.F. All authors have read and agreed to the published version of the manuscript.

**Funding:** This work was supported by the National Natural Science Foundation of China (52002295 and 52172023).

**Institutional Review Board Statement:** Not applicable.

**Informed Consent Statement:** Not applicable.

**Data Availability Statement:** Not applicable.

**Conflicts of Interest:** The authors declare no conflict of interest.

## References

1. Zhao, P.; Dong, P.L. Carbon emission cannot be ignored in future of Chinese steel industry. *Iron Steel* **2018**, *53*, 1–7.
2. Benjamin, N.I.; Lin, B. Quantile analysis of carbon emissions in China metallurgy industry. *J. Clean. Prod.* **2020**, *243*, 118534. [[CrossRef](#)]
3. Tang, J.; Chu, M.S.; Li, F.; Feng, C.; Liu, Z.G.; Zhou, Y.S. Development and progress on hydrogen metallurgy. *Int. J. Min. Met. Mater.* **2020**, *27*, 713–723. [[CrossRef](#)]
4. Tso, S.T.; Pask, J.A. Reaction of fused silica with hydrogen gas. *J. Am. Ceram. Soc.* **1982**, *65*, 457–460. [[CrossRef](#)]
5. Herbell, T.P.; Eckel, A.J.; Hull, D.R.; Misra, A.K. Effect of Hydrogen on the Strength and Microstructure of Selected Ceramics. Available online: <https://ntrs.nasa.gov/api/citations/19910005169/downloads/19910005169.pdf> (accessed on 1 October 2022).
6. Wang, R.R.; Zhang, J.L.; Liu, Y.R.; Zheng, A.Y.; Liu, Z.J.; Liu, X.L.; Li, Z.G. Thermal performance and reduction kinetic analysis of cold-bonded pellets with CO and H<sub>2</sub> mixtures. *Int. J. Min. Met. Mater.* **2018**, *25*, 752–761. [[CrossRef](#)]
7. Klimova, V.; Pakhaluev, V.; Shcheklein, S. On the problem of efficient production of hydrogen reducing gases for metallurgy utilizing nuclear energy. *Int. J. Hydrogen Energy* **2016**, *41*, 3320–3325. [[CrossRef](#)]
8. Zhang, Y.; Yue, Q.; Chai, X.; Wang, Q.; Lu, Y.; Ji, W. Analysis of process parameters on energy utilization and environmental impact of hydrogen metallurgy. *J. Clean. Prod.* **2022**, *361*, 132289. [[CrossRef](#)]
9. Cavaliere, P. Direct reduced iron: Most efficient technologies for greenhouse emissions abatement. In *Clean Ironmaking and Steelmaking Processes*; Springer: Cham, Switzerland, 2019; pp. 419–484.
10. Li, L.; Niu, L.; Guo, H.J.; Duan, S.C.; Li, Y.Q.; Meng, X.L. Experimental research and kinetics analysis on hydrogen reduction of limonite. *Chin. J. Eng.* **2015**, *37*, 13–19.
11. Bai, M.H.; Li, L.Y.; Xu, K.; Han, S.F.; Lu, J.C.; Dong, J.B. Numerical analysis and optimization on hydrogen utilization in DR shaft furnace. *J. Yanshan Univ.* **2016**, *40*, 481–486.
12. Yao, X.; Guo, H.J.; Li, Y.Q.; Sun, G.Y.; Li, L. Direct reduction of magnetite under different reducing conditions by hydrogen. *Nonferrous Met. Sci. Eng.* **2015**, *6*, 12–16.
13. Hamadeh, H.; Mirgoux, O.; Patisson, F. Detailed modeling of the direct reduction of iron ore in a shaft furnace. *Materials* **2018**, *11*, 1865. [[CrossRef](#)] [[PubMed](#)]
14. Sun, G.Y.; Li, B.; Yang, W.S.; Guo, J.; Guo, H.J. Analysis of energy consumption of the reduction of Fe<sub>2</sub>O<sub>3</sub> by hydrogen and carbon monoxide mixtures. *Energies* **2020**, *13*, 1986. [[CrossRef](#)]
15. Xu, C.Y.; Zheng, A.Y.; Zhang, J.L.; Wang, R.R.; Li, Y.; Wang, Y.Z.; Liu, Z.J. Effect of H<sub>2</sub>/CO ratio on gas consumption and energy utilization rate of gas-based direct reduction process. In *Proceedings of the 10th International Symposium on High-Temperature Metallurgical Processing*; Springer: Cham, Switzerland, 2019; pp. 631–647.
16. Guo, X.; Wu, S.; Xu, J.P.; Du, K. Reducing gas composition optimization for COREX®-pre-reduction shaft furnace based on CO-H<sub>2</sub> mixture. *Procedia Eng.* **2011**, *15*, 4702–4706. [[CrossRef](#)]

17. Li, J.L.; Li, F.; Zhu, X.H.; Lin, D.B.; Li, Q.F.; Liu, W.H.; Xu, Z. Colossal dielectric permittivity in hydrogen-reduced rutile TiO<sub>2</sub> crystals. *J. Alloys Compd.* **2017**, *692*, 375–380. [[CrossRef](#)]
18. Chen, W.P.; Wang, Y.; Dai, J.Y.; Lu, S.G.; Wang, X.X.; Lee, P.F.; Chan, H.L.W.; Choy, C.L. Spontaneous recovery of hydrogen-degraded TiO<sub>2</sub> ceramic capacitors. *Appl. Phys. Lett.* **2004**, *84*, 103–105. [[CrossRef](#)]